Real-space cluster dynamical mean-field approach to the Falicov-Kimball model: An alloy-analogy approach

P. Haldar, M. S. Laad, and S. R. Hassan*
Institute of Mathematical Sciences, Taramani, Chennai 600113, India
and Homi Bhabha National Institute Training School Complex, Anushakti Nagar, Mumbai 400085, India
(Received 21 May 2016; revised manuscript received 20 December 2016; published 13 March 2017)

It is long known that the best single-site coherent potential approximation falls short of describing Anderson localization. Here, we study a binary alloy disorder [or equivalently, a spinless Falicov-Kimball (FK)] model and construct a dominantly analytic cluster extension that treats intracluster ($1/d$, d = spatial dimension) correlations *exactly*. We find that, in general, the irreducible two-particle vertex exhibits clear nonanalyticities *before* the band splitting transition of the Hubbard type occurs, signaling onset of an unusual type of localization at strong coupling. Using time-dependent response to a sudden local quench as a diagnostic, we find that the long-time wave-function overlap changes from a power-law to an anomalous form at strong coupling, lending additional support to this idea. Our results also imply such "strong" localization in the equivalent FK model, the simplest *interacting* fermion system.

DOI: 10.1103/PhysRevB.95.125116

I. INTRODUCTION

Anderson's seminal paper [1] spawned the fertile field of localization in disordered systems. While all states in spatial dimension $d = 1,2$ are long known to be localized for any arbitrary disorder in the "weak" localization sense, strong enough disorder is generally expected to lead to exponential localization in all d. In a distinct vein—the *exact* and otherwise successful mean-field theory of Anderson localization (AL)—the coherent potential approximation (CPA) cannot, by construction, describe AL, since it cannot account for coherent backscattering processes that underpin AL. Nevertheless, CPA has been used in the Vollhardt-Wölfle theory to obtain a phase diagram with AL and metallic phases [2]. Other schemes marry the CPA with typical medium theory to study AL [3]. However, given the necessity of including nonlocal correlations, several heavily numeric-based cluster approaches [4–6] have also been devised with mixed success. In addition, the simplest model of correlated fermions on a lattice, the Falicov-Kimball model (FKM), is isomorphic to the binary alloy Anderson disorder model, and exhibits a continuous metal-insulator transition of the Hubbard band splitting type [7]. One might thus expect the above issues to be relevant for the FKM as well. To our knowledge, a dominantly *analytic* approach to cluster-based techniques in such contexts remains to be attempted, and is potentially of great interest.

Recent work on many-body localization [8] suggests that at strong disorder the localization length is of the order of lattice constant ($\xi \simeq 1$). In this limit, an *exact* treatment of intersite "disorder" ($1/d$) correlations beyond dynamical mean-field theory (DMFT) may thus be adequate to describe "strong" localization. Nonlocal response to a sudden local quench (a suddenly switched-on localized hole) in this regime exhibits a statistical orthogonality catastrophe, also studied earlier in the context of correlated impurity potentials in a Fermi gas [9]. Thus, qualitative change in the long-time response of a system to a sudden local quench, wherein the explicit long-time wave-function overlap undergoes a qualitative change at strong disorder, can be a novel diagnostic of strong localization. Can we study how the long-time response to a sudden local quench evolves across the metal-insulator transition (MIT) in the FKM, and can such an endeavor provide deeper insight into strong localization at a continuous metal-insulator transition?

In this paper, we develop an analytic cluster DMFT (CDMFT) for the noninteracting Anderson disorder or FK model

$$H_{AM} = -t \sum_{\langle i,j\rangle,\sigma} (c^{\dagger}_{i\sigma} c_{j\sigma} + \text{H.c.}) + \sum_{i,\sigma} v_i c^{\dagger}_{i\sigma} c_{i\sigma} \qquad (1)$$

on a Bethe lattice. The v_i are random variables with a binary alloy distribution: $P(v_i) = (1-x)\delta(v_i) + x\delta(v_i - U)$, relabeling $v_i = U n_{id}$ where $n_{id} = d^{\dagger}_i d_i$ is the occupation number of a spinless nondispersive fermion state ($n_{id} = 0,1$ for all i). The mapping between the two models implies that the $n_{i,d}$ are randomly distributed according to the above binary alloy distribution. We extend earlier two site cluster DMFT [10] (we use the same notations here as in Ref. [10]), wherein a crucial advance is to go beyond the DMFT-like *site*-local Weiss field to one that explicitly incorporates full intracluster disorder correlations (see below for details) via a matrix Weiss field. This is a nontrivial step, and is necessary to obtain the correct causal *cluster* propagators and self-energies. A unique and very attractive aspect of our CDMFT is that we obtain explicit closed-form expressions for the cluster propagators (thus self-energies and irreducible charge vertices): while H_{AM} is known to be analytically solvable in $d = \infty$ [11], a dominantly analytic cluster extension has remained elusive, though the problem has been tackled numerically [4–6]. Remarkably, one just needs to solve two coupled nonlinear algebraic equations for a two site cluster (N equations for a N-site cluster) leading to extreme computational simplification, even with finite alloy short-range order (SRO). This makes it very attractive for use for real correlated systems in conjunction with multiband DMFT or CDMFT. We will be specifically concerned with studying quantum critical aspects at the the Hubbard type of a continuous MIT accompanied by band splitting. Extensions to

*prosenjit|mslaad|shassan@imsc.res.in

study Anderson localization within the formalism developed in this paper are very interesting, but this is deferred for the future.

II. MODEL AND SOLUTION

The Hamiltonian for the noninteracting Anderson disorder model or equivalently the FKM within alloy-analogy approximation is

$$H = -t \sum_{\langle i,j\rangle,\sigma} (c^{\dagger}_{i\sigma} c_{j\sigma} + \text{H.c.}) + \sum_{i\sigma} v_i n_{i\sigma}. \tag{2}$$

Here, v_i is taken as diagonal disorder with binary distribution, i.e.,

$$P(v_i) = (1-x)\delta(v_i - v_A) + x\delta(v_i - v_B) \tag{3}$$

with $v_A = 0$ and $v_B = U$. We further consider SRO between two nearest-neighbor sites (i,j) as $f_{ij} = \langle v_i v_j\rangle - \langle v_i\rangle\langle v_j\rangle = C$, a constant parameter, although in real materials f_{ij} depends on the x, temperature, and other physical variables and this dependence should be considered explicitly.

We mapped the Hamiltonian using CDMFT technique to an effective Anderson impurity model with impurity as a two site cluster embedding by an effective dynamical bath.

The Hamiltonian for the Anderson impurity model is given as

$$H_{\text{imp}} = -t\sum_{\sigma}(c^{\dagger}_{0\sigma} c_{\alpha\sigma} + \text{H.c.}) + U \sum_{i\in\{0,\alpha\}\sigma} x_i n_{i\sigma} + \sum_{i\in\{0,\alpha\},k,\sigma} (v_{ki} c^{\dagger}_{i\sigma} c_{k\sigma} + \text{H.c.}) + \sum_{k,\sigma} \epsilon_k c^{\dagger}_{k\sigma} c_{k\sigma}. \tag{4}$$

The first term is the hopping between two sites $(0,\alpha)$ of the cluster impurity; the second term corresponds to the interaction of the impurity; the third term describes the hybridization between the impurity and the bath and fourth term describes the dispersive bath. Here, $x_i \equiv n_{id}$ is the occupation of localized fermions in FKM.

The two-site cluster impurity Green's function is given in matrix form:

$$\hat{\mathbf{G}} = \begin{pmatrix} G_{00}(\omega) & G_{\alpha 0}(\omega) \\ G_{\alpha 0}(\omega) & G_{00}(\omega) \end{pmatrix}.$$

Here, the element of $\hat{\mathbf{G}}$ is defined as $G^{\sigma}_{ij}(\omega) := \langle c_{i\sigma}; c^{\dagger}_{j\sigma}\rangle$ with σ the spin indices, i.e., $\sigma \in \{\uparrow,\downarrow\}$.

The equation of motion (EOM) for $G^{\sigma}_{ij}(\omega)$ is

$$\omega G^{\sigma}_{ij}(\omega) = \delta_{ij} - t\sum_{l\neq i} G^{\sigma}_{lj}(\omega) + U\langle x_i c_{i\sigma}; c^{\dagger}_{j\sigma}\rangle + \sum_k v_{ki} G^{\sigma}_{kj}(\omega), \tag{5}$$

where we use the identity for fermions, $\omega\langle \hat{A}; \hat{B}\rangle = \langle [\hat{A}, \hat{B}]_+\rangle + \langle [[\hat{A}, \hat{H}_{\text{imp}}]; \hat{B}]_+\rangle$. Similarly, the EOM for the higher-order Green's function $\langle x_0 c_{i\sigma}; c^{\dagger}_{j\sigma}\rangle$ is

$$\omega\langle x_0 c_{i\sigma}; c^{\dagger}_{j\sigma}\rangle = \langle x_0\rangle\delta_{ij} - t\sum_{l\neq i}\langle x_0 c_{l\sigma}; c^{\dagger}_{j\sigma}\rangle + U\langle x_0 x_i c_{i\sigma}; c^{\dagger}_{j\sigma}\rangle + \sum_k v_{ki}\langle x_0 c_{k\sigma}; c^{\dagger}_{j\sigma}\rangle \tag{6}$$

and the EOM for $\langle x_\alpha c_{i\sigma}; c^{\dagger}_{j\sigma}\rangle$ is

$$\omega\langle x_\alpha c_{i\sigma}; c^{\dagger}_{j\sigma}\rangle = \langle x_\alpha\rangle\delta_{ij} - t\sum_{l\neq i}\langle x_\alpha c_{l\sigma}; c^{\dagger}_{j\sigma}\rangle + U\langle x_\alpha x_i c_{i\sigma}; c^{\dagger}_{j\sigma}\rangle + \sum_k v_{ki}\langle x_\alpha c_{k\sigma}; c^{\dagger}_{j\sigma}\rangle. \tag{7}$$

Again, the EOM for $\langle x_0 x_\alpha c_{i\sigma}; c^{\dagger}_{j\sigma}\rangle$ is

$$(\omega - U)\langle x_0 x_\alpha c_{i\sigma}; c^{\dagger}_{j\sigma}\rangle = \langle x_0 x_\alpha\rangle\delta_{ij} - t\sum_{l\neq i}\langle x_0 x_\alpha c_{l\sigma}; c^{\dagger}_{j\sigma}\rangle + \sum_k v_{ki}\langle x_0 x_\alpha c_{k\sigma}; c^{\dagger}_{j\sigma}\rangle. \tag{8}$$

Here, $\langle x_0 x_\alpha\rangle = \langle x_\alpha x_0\rangle \equiv \langle x_{0\alpha}\rangle$.

The EOM for the $\langle A_{0\alpha} c_{k\sigma}; c^{\dagger}_{j\sigma}\rangle$ is

$$(\omega - \epsilon_k)\langle A_{0\alpha} c_{k\sigma}; c^{\dagger}_{j\sigma}\rangle = \sum_i v^{*}_{ki}\langle A_{0\alpha} c_{i\sigma}; c^{\dagger}_{j\sigma}\rangle. \tag{9}$$

Here, $A_{0\alpha} \equiv 1, x_0, x_\alpha, x_{0\alpha}$.

We derive the generalized form of the cluster Green's function by solving Eqs. (5)–(9):

$$G_{ij}(\omega) = \left[\frac{1 - \langle x_0\rangle - \langle x_\alpha\rangle + \langle x_{0\alpha}\rangle}{\xi_2(\omega)} + \frac{\langle x_0\rangle - \langle x_{0\alpha}\rangle}{\xi_2(\omega) - U}\right] \times \left[\delta_{ij} - \frac{F_2(\omega)}{[t - \Delta_{\alpha 0}(\omega)]}(1-\delta_{ij})\right] + \left[\frac{\langle x_\alpha\rangle - \langle x_{0\alpha}\rangle}{\xi_1(\omega)} + \frac{\langle x_{0\alpha}\rangle}{\xi_1(\omega) - U}\right] \times \left[\delta_{ij} - \frac{F_1(\omega)}{[t - \Delta_{\alpha 0}(\omega)]}(1-\delta_{ij})\right]. \tag{10}$$

Here, $\xi_1(\omega) = [\omega - \Delta_{00}(\omega) - F_1(\omega)]$, $\xi_2(\omega) = [\omega - \Delta_{00}(\omega) - F_2(\omega)]$, $F_1(\omega) \equiv \frac{[t-\Delta_{\alpha 0}(\omega)]^2}{\omega - \Delta_{00}(\omega) - U}$, and $F_2(\omega) \equiv \frac{[t-\Delta_{\alpha 0}(\omega)]^2}{\omega - \Delta_{00}(\omega)}$. We obtain renormalized $\xi_{1(2)}$ and t in the diagonal Green's function $[G_{00}(\omega)]$ as compared with the results of Ref. [10]. $\xi_{1(2)}$ and t are renormalized by $\tilde{\xi}_{1(2)} = [\xi_{1(2)} - \Delta_{00}(\omega)]$ and $\tilde{t} = [t - \Delta_{\alpha 0}(\omega)]$, respectively. The bath function $\hat{\mathbf{\Delta}}(\omega)$ in the two site cluster model is a 2×2 matrix:

$$\hat{\mathbf{\Delta}}(\omega) = \begin{pmatrix} \Delta_{00}(\omega) & \Delta_{\alpha 0}(\omega) \\ \Delta_{\alpha 0}(\omega) & \Delta_{00}(\omega) \end{pmatrix}.$$

Here, $\hat{\mathbf{\Delta}}(\omega)$ is computed from matrix generalization of the dynamic Weiss field [11]:

$$G(\omega) = \int_{-W}^{+W} \frac{\rho_0(\epsilon) d\epsilon}{G^{-1}(\omega) + \Delta(\omega) - \epsilon}, \tag{11}$$

where $\rho_0(\epsilon)$ is the unperturbed DOS.

III. GENERAL FORMALISM FOR THE TWO SITE CLUSTER METHOD

We can also exactly estimate the cluster irreducible vertex functions and (charge) susceptibility by generalizing the well-known procedure employed in DMFT studies [11]. It

turns out that exploiting cluster symmetry is particularly useful in this instance, and markedly simplifies the analysis. The solution of the two site cluster impurity problem gives the following matrix Green's function and the self-energy:

$$\hat{\mathbf{G}} = \begin{pmatrix} G_{00} & G_{\alpha 0} \\ G_{\alpha 0} & G_{00} \end{pmatrix}, \quad \hat{\Sigma} = \begin{pmatrix} \Sigma_{00} & \Sigma_{\alpha 0} \\ \Sigma_{\alpha 0} & \Sigma_{00} \end{pmatrix}.$$

To go over to a representation where these matrices are diagonal in the cluster momenta, $\mathbf{K}$ points $K_I = (0,0,\ldots)$ and $K_{II} = (\pi,\pi,\ldots)$, we divide the Brillouin zone into two subzones as done in CDMFT studies for the Hubbard model [12]. For brevity, we label regions I and II by S and P, respectively. Now, self-energy and Green's-function matrices take on the diagonalized forms

$$\hat{\mathbf{G}} = \begin{pmatrix} G_S & 0 \\ 0 & G_P \end{pmatrix}, \quad \hat{\Sigma} = \begin{pmatrix} \Sigma_S & 0 \\ 0 & \Sigma_P \end{pmatrix},$$

where

$$G_S = G_{00} + G_{\alpha 0}, \quad G_P = G_{00} - G_{\alpha 0}$$

and

$$\Sigma_S = \Sigma_{00} + \Sigma_{\alpha 0}, \quad \Sigma_P = \Sigma_{00} - \Sigma_{\alpha 0}$$

with

$$G_{S(P)}(\omega) = \int \frac{\rho^0_{S(P)}(\epsilon) d\epsilon}{\omega + \mu - \epsilon - \Sigma_{S(P)}}. \tag{12}$$

The partial density of states, which are now nothing other than the $\mathbf{K}$-dependent spectral functions, are given by

$$\rho^0_{S(P)}(\epsilon) = 2 \times \int_{\mathbf{k} \in S(P)} d\mathbf{k} \delta(\epsilon - \epsilon_k). \tag{13}$$

In this representation, it turns out to be easier to compute the irreducible vertex functions. Specifically, the *only* quantity relevant for the disorder problem is the irreducible particle-hole (p-h) vertex function $\hat{\Gamma}$ given as $\hat{\Gamma} = \frac{\delta \hat{\Sigma}}{\delta \hat{\mathbf{G}}}$ (the "spin fluctuation" and "pairing" vertex appear in the FKM, but are irrelevant for the disorder problem). Since both self-energy and Green's-function matrices are diagonal in the $S(P)$ basis, the vertex function is separable with respect to the S or P channel as well:

$$\Gamma_{S(P)} = \frac{\delta \Sigma_{S(P)}}{\delta G_{S(P)}}. \tag{14}$$

IV. CALCULATION OF CHARGE SUSCEPTIBILITY

With explicit knowledge of the p-h irreducible vertex as above, the momentum-dependent susceptibility corresponding to the $S(P)$ channels is evaluated using the Bethe-Salpeter equation:

$$\begin{aligned} &\chi_{S(P)}(\mathbf{q}, i\omega_m, i\omega_n; i\nu_l) \\ &= \chi^0_{S(P)}(\mathbf{q}, i\omega_m; i\nu_l)\delta_{mn} - T \sum_{n'} \chi^0_{S(P)}(\mathbf{q}, i\omega_m; i\nu_l) \\ &\quad \times \Gamma_{S(P)}(i\omega_m, i\omega_{n'}; i\nu_l) \chi_{S(P)}(\mathbf{q}, i\omega_{n'}, i\omega_n; i\nu_l). \end{aligned} \tag{15}$$

To make progress, we proceed along lines similar to those adopted in DMFT studies [11].

(i) The full susceptibility is found by summing over the fermionic Mastubara frequencies, $\chi_{S(P)}(\mathbf{q}, i\nu_l) = T \sum_{mn} \chi_{S(P)}(\mathbf{q}, i\omega_m, i\omega_n; i\nu_l)$.

(ii) The vertex functions $\Gamma_{S(P)}(i\omega_m, i\omega_{n'}; i\nu_l)$ are evaluated as

$$\Gamma_{S(P)}(i\omega_n, i\omega_m; i\nu_l) = \frac{1}{T} \frac{\Sigma^{S(P)}_n - \Sigma^{S(P)}_{n+l}}{G^{S(P)}_n - G^{S(P)}_{n+l}} \delta_{m,n}. \tag{16}$$

As $\chi_{S(P)}$ are diagonal in the S or P channel, we keep only the channel index S, with the understanding that an identical calculation holds for the P channel. Using Γ from Eq. (27) we find

$$\begin{aligned} &\chi^S(\mathbf{q}, i\omega_m, i\omega_n; i\nu_l) \\ &= \chi^S_0(\mathbf{q}, i\omega_m; i\nu_l)\delta_{mn} - T \chi^S_0(\mathbf{q}, i\omega_m; i\nu_l) \\ &\quad \times \Gamma^S(i\omega_m, i\omega_m; i\nu_l) \chi^S(\mathbf{q}, i\omega_m, i\omega_n; i\nu_l) \end{aligned} \tag{17}$$

$$\Rightarrow \chi^S(\mathbf{q}, i\omega_m, i\omega_n; i\nu_l) = \frac{\chi^S_0(\mathbf{q}, i\omega_m; i\nu_l)\delta_{mn}}{1 + \chi^S_0(\mathbf{q}, i\omega_m; i\nu_l) \frac{\Sigma^S_m - \Sigma^S_{m+l}}{G^S_m - G^S_{m+l}}}. \tag{18}$$

(iii) Now, the full lattice susceptibility with $\mathbf{q}$ replaced by $X(\mathbf{q})$ is given by

$$\begin{aligned} \chi^S(X, i\nu_l \neq 0) &= T \sum_{m,n} \chi^S(X, i\omega; i\nu_l) \\ &= T \sum_{m,n} \frac{\chi^S_0(X, i\omega_m; i\nu_l)\delta_{mn}}{1 + \chi^S_0(X, i\omega_m; i\nu_l) \frac{\Sigma^S_m - \Sigma^S_{m+l}}{G^S_m - G^S_{m+l}}} \end{aligned} \tag{19}$$

where $X(\mathbf{q}) = \lim_{d\to\infty} \sum_{i=1}^{d} \cos(\frac{q_i}{d})$

$$\Rightarrow \chi^S(X, i\nu_l \neq 0) = T \sum_{m} \frac{\chi^S_0(X, i\omega_m; i\nu_l)}{1 + \chi^S_0(X, i\omega_m; i\nu_l) \frac{\Sigma^S_m - \Sigma^S_{m+l}}{G^S_m - G^S_{m+l}}}. \tag{20}$$

(iv) For $\mathbf{q} = 0 (X = 1)$, we find that

$$\chi(1; i\nu_l \neq 0) = -T \sum_{m} \frac{G_m - G_{m+l}}{i\nu_l} = 0. \tag{21}$$

This just reflects conservation of the total c-fermion number, and thus vanishes by symmetry.

(v) For generic $\mathbf{q}(X = 0)$, we calculate the sum over Matsubara frequency by contour integration. The bare susceptibility for $X = 0$ is given as $\chi^S_0(0, i\omega_m; \nu_l) = -G^S_m G^S_{m+l}$

$$\Rightarrow \chi^S(X = 0, i\nu_l \neq 0) = -T \sum_{m} \frac{G^S_m G^S_{m+l}}{1 - G^S_m G^S_{m+l} \frac{\Sigma^S_m - \Sigma^S_{m+l}}{G^S_m - G^S_{m+l}}}. \tag{22}$$

As mentioned before, a similar analysis holds for the P channel at every step in the procedure above.

After performing analytical continuation from Matsubara frequency to real frequency in the standard way, the final expression for the susceptibility corresponding to the S or P channel becomes

$$\chi_{S(P)}(X=0,\nu\neq 0) = \frac{1}{2\pi i}\int_{-\infty}^{\infty} d\omega \Bigg\{ f(\omega)\frac{G_{S(P)}(\omega)G_{S(P)}(\omega+\nu)}{1-G_{S(P)}(\omega)G_{S(P)}(\omega+\nu)[\Sigma_{S(P)}(\omega)-\Sigma_{S(P)}(\omega+\nu)]/(G_{S(P)}(\omega)-G_{S(P)}(\omega+\nu))} - f(\omega+\nu)\frac{G^*_{S(P)}(\omega)G^*_{S(P)}(\omega+\nu)}{1-G^*_{S(P)}(\omega)G^*_{S(P)}(\omega+\nu)[\Sigma^*_{S(P)}(\omega)-\Sigma^*_{S(P)}(\omega+\nu)]/(G^*_{S(P)}(\omega)-G^*_{S(P)}(\omega+\nu))} - [f(\omega)-f(\omega+\nu)]\frac{G^*_{S(P)}(\omega)G_{S(P)}(\omega+\nu)}{1-G^*_{S(P)}(\omega)G_{S(P)}(\omega+\nu)[\Sigma^*_{S(P)}(\omega)-\Sigma_{S(P)}(\omega+\nu)]/[G^*_{S(P)}(\omega)-G_{S(P)}(\omega+\nu)]} \Bigg\} \quad (23)$$

where we have replaced the retarded Green's function $G^R_{S(P)}$ by $G_{S(P)}$ and the advanced Green's function $G^A_{S(P)}$ by the complex conjugate of the retarded Green's function $G^*_{S(P)}$.

The procedure (i)–(v) allows us to *exactly* estimate the cluster p-h irreducible vertices and the charge susceptibility in the FKM to $O(1/d)$.

V. RESULTS

A. One-particle spectral response

We now present our results. We work with a semicircular unperturbed density of states (DOS) as appropriate for a Bethe lattice in high d, given by $\rho_0(\epsilon) = (2/\pi D)\sqrt{D^2-\epsilon^2}$ where $D = 2t = 1$ is the c-fermion half-bandwidth. We begin with a "particle-hole symmetric" case with $\langle n_{ic}\rangle = 1/2$ and a probability distribution $P(v_i) = 1/2[\delta(v_i)+\delta(v_i-U)]$ or in the FKM context with a half-filled c-fermion band. In Fig. 1, we show the local DOS (LDOS) as U is increased through a critical $U_c = 1.8$, where a *continuous* MIT of the Mott-Hubbard type occurs via the Hubbard band splitting. Comparing with the exact DMFT solution [11], we see that incorporation of dynamical effects of $1/d$ correlations in our two site CDMFT gives rise to additional features in the LDOS. These features arise from repeated scattering of the electrons off spatially separated scattering centers and are visible even for the totally random case, defined as $f_{0\alpha} = \langle x_0 x_\alpha\rangle - \langle x_0\rangle\langle x_\alpha\rangle = 0$. In the lower panel, we show the LDOS for the asymmetric FKM, with $\langle n_{i,d}\rangle = \langle x_i\rangle = 0.45$, wherein loss of particle-hole symmetry is faithfully reflected as an asymmetric LDOS. It is clear that the MIT is associated with a genuine quantum critical point (QCP). The advantage of CDMFT is that cluster *spectral* functions, defined as $A(\mathbf{K},\omega)$ with $\mathbf{K} = (0,0),(\pi,\pi)$, can be explicitly read off. In Fig. 2, we exhibit $A(\mathbf{K},\omega)$ as a function of U. It is obvious that $\rho_S(\omega) = A(\mathbf{K}=(0,0),\omega) = \rho_P(-\omega) = A(\mathbf{K}=(\pi,\pi),-\omega)$ for the particle-hole symmetric case, as it must be. For the Bethe lattice, we find that the LDOS $\rho(\omega) = C|\omega|^{1/3}$ (shown in Fig. 4) exactly at the QCP ($U_c = 1.8$), a result similar to that found for the same model in DMFT [13]. The spectral functions also exhibit these singular features, albeit in a $\mathbf{K}$-dependent fashion. Notwithstanding these similarities, we stress that our extension of DMFT faithfully captures

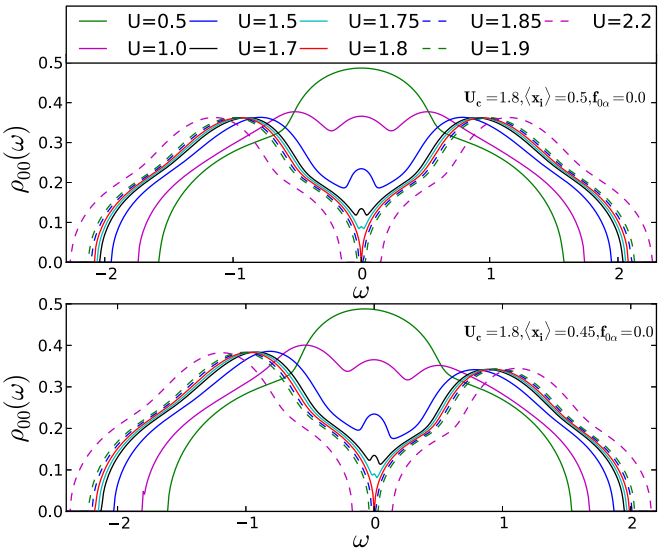

FIG. 1. The local density of states (LDOS) of the binary alloy disorder model for p-h symmetry (upper panel) and p-h asymmetric case (lower panel). A clear continuous band splitting transition of the Hubbard (or Falicov-Kimball model-like) variety is seen in both cases. At $U_c = 1.8$ (red curve), the LDOS exhibits a critical $|\omega|^{1/3}$ singular behavior in both cases.

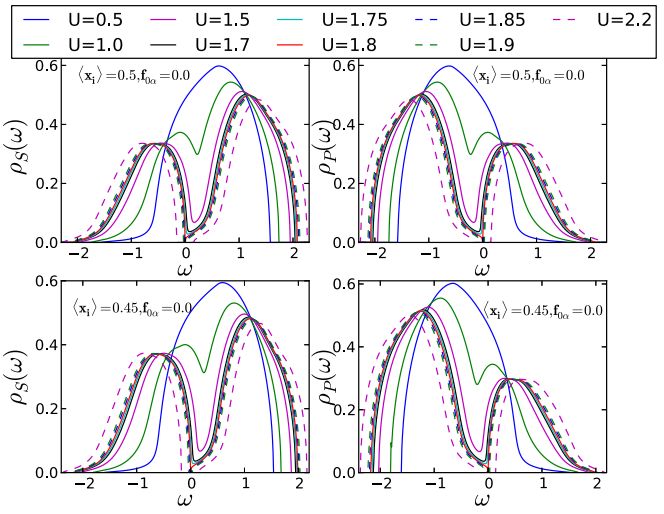

FIG. 2. The cluster-momentum resolved one-electron spectral functions for the same parameters as in Fig. 1. For the p-h symmetric case, the symmetry relation $\rho_S(\omega) = \rho_P(-\omega)$ is clearly satisfied as it must be (upper panel).

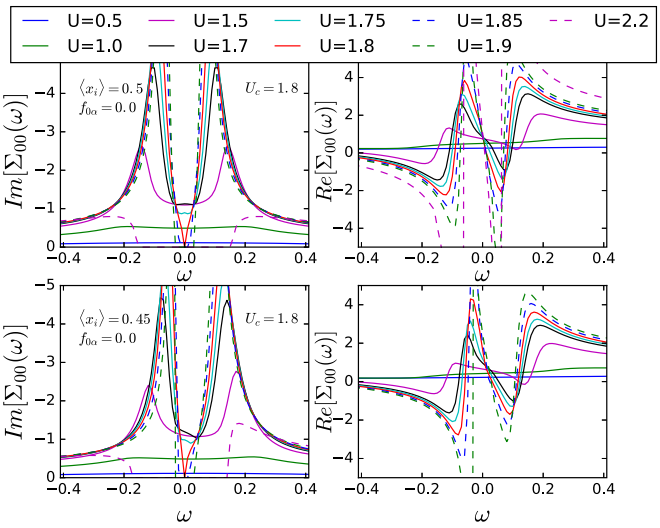

FIG. 3. $\Sigma_{00}(\omega)$ (both real and imaginary part) vs U for the binary-alloy disorder problem for the same parameters as in Fig. 1. For small U, our results agree with self-consistent Born approximation [constant $\mathrm{Im}\Sigma_{00}(\omega)$]. As U increases, $\mathrm{Im}\Sigma_{00}(\omega)$ develops marked low-energy structure, and at $U_c = 1.8$ (red curve), $\mathrm{Im}\Sigma_{00}(\omega) \simeq |\omega|^{1/3}$, reflecting the nonperturbative nature of the "Hubbard III" quantum criticality. The $\mathrm{Re}\Sigma_{00}(\omega)$ shows discontinuity at $\omega = 0$ at the critical U.

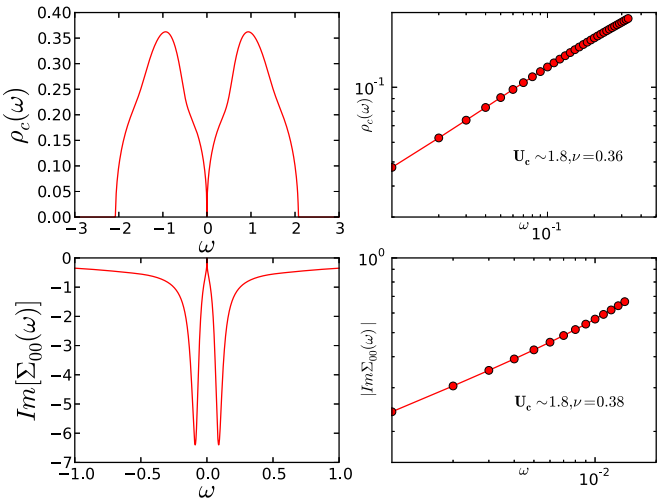

FIG. 4. Exponent of $\rho_{00}(\omega)$ and $\mathrm{Im}\Sigma_{00}(\omega)$ closed to the Fermi energy at critical value of U with symmetric alloy.

the feedback of the nonlocal (intracluster) correlations on the single-particle DOS and the self-energies (see below) in contrast to DMFT, where such $1/d$ feedback effects are absent. In the left panels of Fig. 3, we exhibit the imaginary part of the cluster-local self-energy, $\mathrm{Im}\Sigma_{00}(\omega)$ for the same parameter values as above. For small U, $\mathrm{Im}\Sigma_{00}$ weakly depends on ω, and is sizable only near $\omega = 0$. However, it has the *wrong* sign, i.e., a minimum, instead of a maximum characteristic of a Landau Fermi liquid, at $\omega = 0$. Thus, the metallic state is incoherent and *not* a Landau Fermi liquid. This is again a feature in common with DMFT studies. In DMFT, it is well known that this feature becomes more prominent as U increases, and diverges at the MIT [11]. In CDMFT, however, $\mathrm{Im}\Sigma_{00}$ develops marked structure already at $U = 1.0$: it develops a maximum at $\omega = 0$, which progressively sharpens up with increasing U in the incoherent metallic regime. Interestingly, right at U_c (red curve), $\mathrm{Im}\Sigma_{00}(\omega) = c|\omega|^{1/3}$ (shown in Fig. 4), reminiscent of what is expected in a *power-law liquid*, in strong contrast to what happens in DMFT, where it diverges. The real part of local self-energy [$\mathrm{Re}\Sigma_{00}(\omega)$] is shown in the right panels of Fig. 3. For the p-h symmetric case (shown in the upper right panel of Fig. 3), $\mathrm{Re}\Sigma_{00}(\omega)$ is $U/2.0$ at ω=0 for all values of U. If we see $\mathrm{Re}[\Sigma_{00}(\omega)] - \frac{U}{2}$ it changes sign according to the ω near the Fermi level and at the transition point ($U \sim U_c$) it shows steep discontinuity at $\omega = 0$. The source of gap opening comes from the divergence of $\frac{\partial}{\partial\omega}\mathrm{Re}\Sigma_{00}(\omega)$ at $\omega = 0$. For $U > U_c$, opening up of a "Mott" gap in the LDOS goes hand in hand with the divergence of $\frac{\partial}{\partial\omega}\mathrm{Re}\Sigma_{00}(\omega)$ and vanishing $\mathrm{Im}\Sigma_{00}(\omega)$ in the gap. In all cases, we also find power-law falloff in self-energies at high energy and, more interestingly, clear isosbestic points [where $\mathrm{Im}\Sigma_{00}(\omega)$ is independent of ω] at $\Omega = \pm 0.2t$. We also find (see lower panels of Fig. 3) that moving away from p-h symmetry does not qualitatively change the above features.

Finally, CDMFT allows a direct evaluation of the **K**-dependent self-energies, which we exhibit in Figs. 5 and 6. As a cross-check, we find that $\mathrm{Im}\Sigma(\mathbf{K} = (0,0),\omega) = \mathrm{Im}\Sigma(\mathbf{K} = (\pi,\pi), -\omega)$, as required by particle-hole (p-h) symmetry for $\langle n_{i,d}\rangle = 0.5$.

In Fig. 7, we exhibit the imaginary parts of the cluster-momentum-resolved irreducible particle-hole vertex functions as functions of U. It is clear that both $\mathrm{Im}\Gamma(\mathbf{K},\omega)$ with $\mathbf{K} = (0,0)$ (called "S") and with $\mathbf{K} = (\pi,\pi)$ (called "P") show nonanalyticities precisely at $\omega = 0$ at $U_c = 1.8$ (red curves). Thus, for the completely random case, we find, as expected, that the "Mott" QCP is signaled by a clear nonanalyticity in the momentum-dependent (irreducible) p-h vertices at the

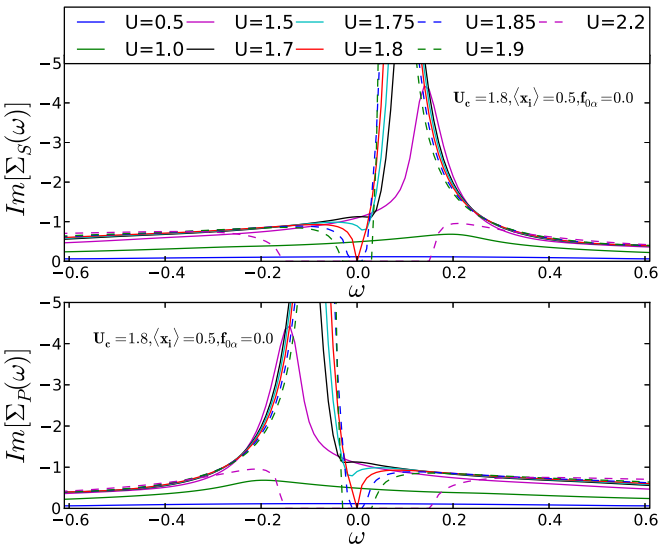

FIG. 5. Same as Fig. 3, but now for the cluster-momentum resolved self-energies. It is clear that the symmetry relation $\mathrm{Im}\Sigma_S(\omega) = \mathrm{Im}\Sigma_P(-\omega)$ holds in the p-h symmetric case.

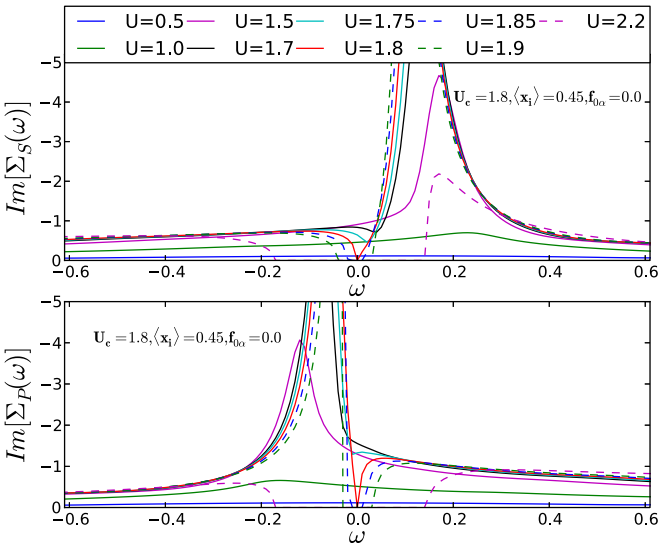

FIG. 6. Same as in Fig. 5, but for the p-h asymmetric case. Though no symmetry is expected nor found here, the critical features are unaffected, since $\mathrm{Im}\Sigma_{S,P}(\omega)$ indeed exhibit the same nonanalytic feature ($\simeq|\omega|^{1/3}$ behavior) for $\omega<0(S)$ and $\omega>0(P)$.

Fermi energy ($\omega=0$). This nonanalytic feature goes hand in hand with a power-law variation of $\mathrm{Im}\Sigma_{S(P)}(\omega)$ in the vicinity of the Fermi energy ($\omega=0$). Along with spectral functions and self-energies, the vertex functions also satisfy the "symmetry" relation, $\mathrm{Im}\Gamma(\mathbf{K}=(0,0),\omega)=-\mathrm{Im}\Gamma(\mathbf{K}=(\pi,\pi),-\omega)$ for the p-h symmetric case. Clearly, the anomalous infra-red behavior of the irreducible vertices is directly related to the clear nonanalytic structures in the cluster self-energies discussed above.

Additional notable features characteristic of $1/d$ effects captured by CDMFT become apparent upon repeating the

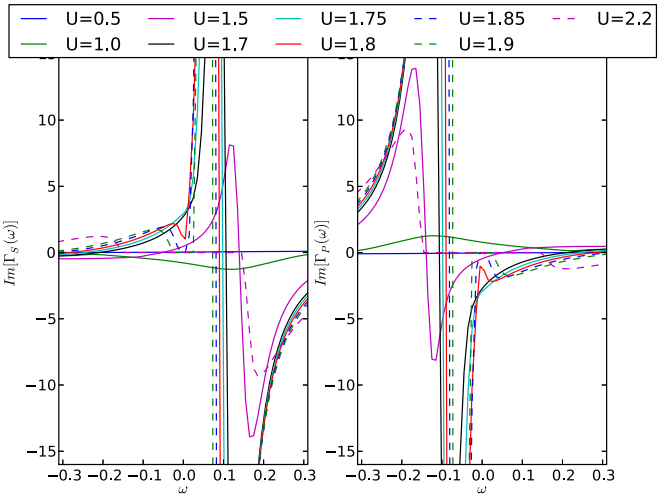

FIG. 7. Imaginary parts of the irreducible particle-hole vertex functions in the S,P channels as a function of U for the binary alloy disorder model. Clear nonanalyticities in $\Gamma_{S,P}(\omega)$ at $\omega=0$ occur precisely at $U_c=1.8$ (red curve), where the continuous Hubbard band splitting transition occurs. In addition, the results confirm the symmetry $\mathrm{Im}\Gamma_S(\omega)=-\mathrm{Im}\Gamma_P(-\omega)$.

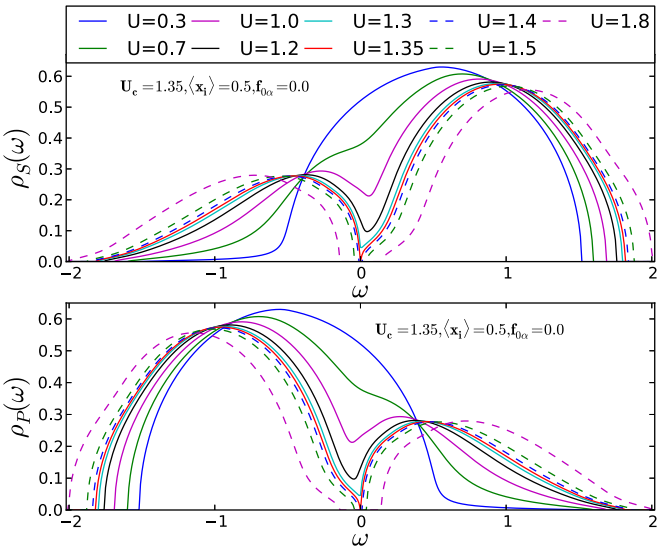

FIG. 8. Cluster-momentum resolved one-electron spectral functions as a function of U for the short-range ordered binary alloy in the p-h symmetric case. As expected, the continuous "Hubbard" transition is now obtained at a smaller $U_c=1.35$ (red curve), due to enhanced suppression of itinerance by the "anti-ferro" alloy short-range order ($f_{0\alpha}=-0.15<0$). As for the totally random alloy, the symmetry relation for the spectral functions still holds. The LDOS shows very similar quantum-critical singular features at low energy at U_c.

above procedure for the case of finite "alloy" SRO, namely, when $f_{0\alpha}=\langle x_0 x_\alpha\rangle-\langle x_0\rangle\langle x_\alpha\rangle\neq 0$.

In Figs. 8–10, we exhibit the cluster spectral functions, self-energies, and p-h vertices for the case of $f_{0\alpha}=-0.15$, which represents the physical situation with short-range "antiferro" alloy correlations on the two site cluster. Now, the MIT occurs at a critical $U_{c1}=1.35$, smaller than for the completely random case. The reason is simple: on very general grounds, short-ranged antiferro alloy correlations suppress the one-electron hopping by a larger amount compared to the random case (this is also reflected in the deeper pseudogap in the incoherent metal for $f_{0\alpha}<0$), simply because the probability for an electron to hop onto its neighbor on the cluster is reduced when there is more probability of having a local potential U on the neighboring site. In this case, $\mathrm{Im}\Sigma(\mathbf{K},\omega)$ shows, on first glance, a behavior similar to the case with $f_{0\alpha}=0$ described before. Upon closer scrutiny of Fig. 9, however, we find that $\mathrm{Im}\Sigma(\mathbf{K},\omega)$ already *diverges* for $U=1.3$, slightly *before* Hubbard band splitting occurs (cyan curve). Also, Fig. 9 also clearly shows the power-law divergence of the self-energy (cyan and red curves), with $\mathrm{Im}\Sigma_{00}(\omega)\simeq|\omega|^{-\eta}$, with $\eta=1/3$ at the MIT. This feature is very different from the pole divergence of the self-energy in the Hubbard model within DMFT, but is indeed seen in the DMFT solution for the FKM when the self-energy and the vertex function are treated consistently at the local level [14]. A related nonanalyticity in $\mathrm{Im}\Gamma(\mathbf{K},\omega)$ also correspondingly occurs at precisely the same value in Fig. 10. Thus, in this case, we find that the irreducible p-h vertex diverges before the actual MIT occurs. Such features are also known for the $d=2$ Hubbard model within the dynamical vertex approximation [15]. However,

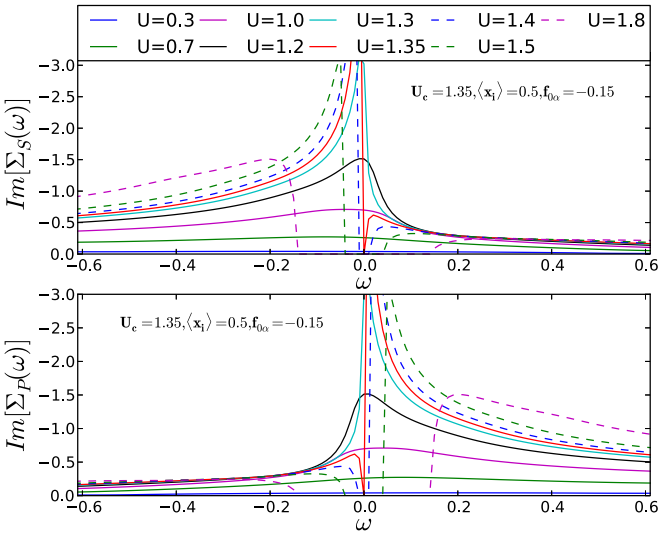

FIG. 9. Imaginary parts of the cluster-momentum resolved one-particle self-energies as a function of U for the short-range ordered binary alloy. The symmetry relation for the cluster self-energies still holds, as does the fact that both show critical power-law behavior at U_c (see text).

this divergence of the vertex function is *not* associated with $[\frac{\partial}{\partial\omega}\mathrm{Re}\Sigma_{00}(\omega)]_{\omega=0} = \infty$, where the actual "Mott" transition occurs. Thus, it is not connected to any symmetry breaking (which would require a divergence in the momentum channel), nor does it lead to nonanalyticities in the one-particle response (the LDOS remains smooth for all $U < U_{c1} = 1.35$).

Thus, at the level of spectral functions and self-energies, our CDMFT for the FKM finds universal features at a quantum-critical Mott transition that are qualitatively similar to those found by Janis and Pokorny [14]. We find that the infrared nonanalytic behavior in $\Gamma(\mathbf{K},\omega)$ *precedes* the MIT.

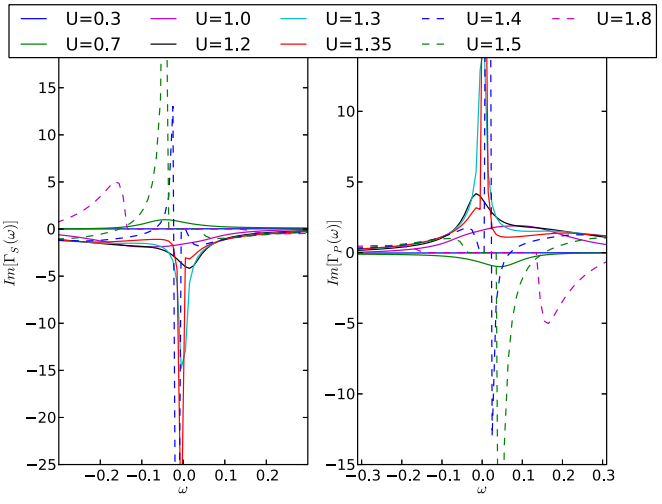

FIG. 10. Imaginary parts of the cluster-momentum resolved irreducible p-h vertex functions for the p-h symmetric short-range ordered binary alloy as a function of U. Clear nonanalyticities in both $\Gamma_{S,P}(\omega)$ occur slightly *before* the Hubbard-type band splitting transition occurs, signifying the onset of a novel kind of localization (see text).

This was probably to be expected, since both approaches deal with quasilocal quantum criticality suited to the Mott-Hubbard problem. The advantages of our extension relate to (i) having a CDMFT that always respects causality [10] and (ii) enabling computation of momentum-resolved spectral responses, even for the hitherto scantily considered cases of explicit "alloy" short-range order. Importantly, having an almost analytic cluster extension of DMFT means that we have to simply deal with N coupled nonlinear algebraic equations to compute the full CDMFT propagators for a N-site cluster, even with short-range order. This is an enormous numerical simplification when one envisages its use for *real* disordered systems, with or without strong Hubbard correlations: these issues have long been extremely well studied using the CPA and DMFT [16]. We anticipate wide uses of such a semianalytic approach as ours in this context.

It is interesting to compare our results to those obtained by Shinaoka and Imada [17]. Motivated by disordered and correlated systems near a MIT, they consider a disordered Hubbard model, where Hubbard correlations are treated within static Hartree-Fock (HF), giving rise to local moments, while disorder effects over and above HF are studied by exact diagonalization techniques. Their main findings are (i) a "soft" gap arises even with purely local interactions, in contrast to that in an Efros-Shklovskii picture, where it arises from long-range coulomb interactions, and (ii) while the LDOS $A(E) \simeq |E - E_F|^\alpha$ with $0.5 < \alpha < 1$ for $|E - E_F| > 0.1$, they see that $A(E) \simeq \exp[-(-\gamma \log|E - E_F|)^3]$ provides a much better fit for $|E - E_F| < 0.1$. In contrast, we find that the LDOS $\rho(\omega) \simeq C|\omega|^{1/3}$ remains valid up to lowest energies at the QCP: this is similar to the situation found in single-site DMFT [13], where precisely the same behavior is found analytically.

These differences could arise from many factors: (a) there are *no* localized magnetic moments in our case, since we do not have the Hubbard term, and (b) while we focus on predominantly short-range disorder correlations, Shinaoka and Imada [17] include longer-range disorder correlations. It is noteworthy that a "soft power-law gap" already appears in CDMFT studies, and while it is conceivable that the low-energy behavior may change upon increasing cluster size, this remains to be shown. Alternatively, if local moments *are* crucial to obtain this behavior, one must study the disordered Hubbard model within CDMFT. This ambitious enterprise is left for future consideration.

B. Charge susceptibility and response to a sudden local quench

In addition to universal critical features found in the last section within an exact-to-$O(1/d)$ CDMFT for the FKM, additional details regarding the nature of this strong-coupling Mott transition can be gleaned from examination of the two-particle response. In particular, the dynamic charge susceptibility of the FKM can also be precisely computed in our approach by using the CDMFT propagators $[G_{S(P)}(\mathbf{k},\omega)]$ and the irreducible p-h vertices $\Gamma_{S(P)}(\omega)$ (notice that the latter have dependence on the cluster momenta $\mathbf{K}$) in the Bethe-Salpeter equation, as detailed in the "Model and Solution" section.

In Fig. 11, we show the imaginary part of the full cluster-local dynamical charge susceptibility as U increases. On first

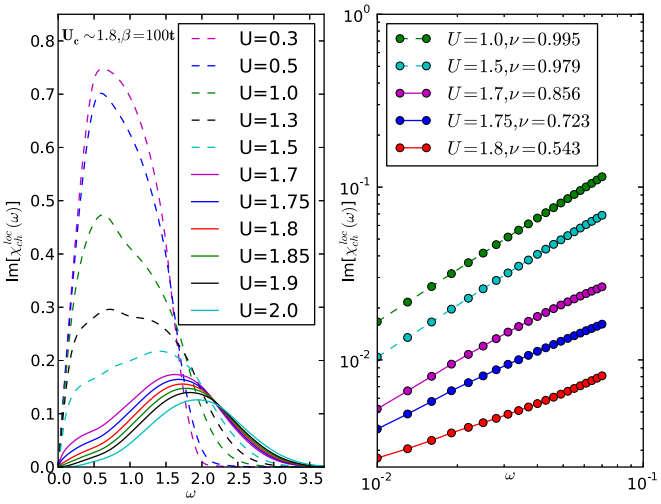

FIG. 11. The imaginary part of the local component of the full dynamical charge susceptibility for the p-h symmetric binary alloy disorder model in the totally random case ($f_{0\alpha} = 0$). Up to $U_1 = 1.4$, $\mathrm{Im}\chi^{\mathrm{loc}}_{ch}(\omega) \simeq \omega$, similar to its DMFT counterpart. However, for $1.5 \leqslant U \leqslant U_c = 1.8$, $\mathrm{Im}\chi^{\mathrm{loc}}_{ch}(\omega) \simeq \omega^{\nu}$ where $\nu = 1 - \kappa$ and $0 < \kappa(U) < 1$ and κ reduces with increasing U, reaching a value $\kappa = 0.5$ at U_c (red curve). This has very unusual consequences for the long-time response to a "sudden" local quench at strong coupling (see text).

glance, our results are quite similar to those in earlier DMFT work [11]. Beginning from small U up to $U \simeq 1.2$, $\mathrm{Im}\chi_{ch}(\omega)$ varies linearly with ω in the infrared, with a maximum at intermediate energy, followed by a high-energy falloff. However, closer scrutiny of the strong-coupling ($U \geqslant 1.4$) regime reveals that this behavior undergoes a qualitative change at low energies: now $\mathrm{Im}\chi_{ch}(\omega) \simeq \omega^{\nu}$, with $\nu = 1 - \kappa$ and $0 < \kappa(U) < 1$. It is important to notice that the configurationally averaged DOS does *not* show any nonanalyticities in this regime, and the system is close to but not in the Mott insulating regime. A closer look at the behavior of the cluster self-energies and irreducible vertex functions in this regime shows that both begin to acquire nontrivial energy dependence at low energy when U is close to the critical value needed for the Mott transition to occur. In fact, as described before, both $\mathrm{Im}\,\Gamma_{S(P)}(\omega)$ start exhibiting strong ω dependence, especially near $\omega = 0$, when $U \geqslant 1.4$, and clear nonanalyticities accompanied by anomalous power-law variation near $\omega = 0$ when one is very close to the transition in the range $1.7 < U < 1.8$. Thus, it is clear that the anomalous low-energy behavior of the collective charge fluctuations is linked to the strong ω dependence and impending nonanalytic behavior in the cluster irreducible vertex as the MIT is approached from the metallic side. Thus, while the fact that the vertex diverges *before* the actual MIT does not lead to nonanalyticity in the one-electron spectral functions, it does qualitatively modify the collective density fluctuations, reflecting in an anomalously overdamped critical form. We are unaware of such a connection existing within earlier DMFT studies [11].

One interpretation of this unusual feature is the following. Close to the Hubbard band splitting (Mott) transition, one generically expects formation of excitons. A simple way to understand this is in terms of the "holon-doublon" mapping of the model, which is a partial particle-hole transformation where $c^{\dagger} \to c^{\dagger}, d \to d^{\dagger}$. Now $U \sum_i n_{i,c} n_{i,d} \to -U \sum_i (n_{i,c} n_{i,d} - n_{i,c})$, whereby the c,d fermions experience an on-site *attraction*, leading to formation of local "pair" bound states (these are excitons in the original model) of the type $\langle c_i^{\dagger} d_i^{\dagger} \rangle$. Quite generally, in a Hubbard model, one expects these bosons to Bose condense. An upshot thereof is the well-known fact that this is nothing else but antiferromagnetic magnetic order, now interpreted as a Bose condensate of spin excitons. In our simplified FKM or binary alloy case, however, such a Bose-Einsten condensate is explicitly forbidden by the fact that the *local* Z_2 gauge symmetry, associated with $[n_{i,d}, H] = 0$ for all i, cannot be spontaneously broken by Elitzur's theorem. This still leaves open the possibility of having intersite excitonic pairing of the c fermions on the two site cluster. Without global broken symmetry, such a state would be a dynamically fluctuating excitonic liquid. One would expect that a phase transition to a "solid" of such excitonic pairs will eventually occur, perhaps as a Berezinskii-Kosterlitz-Thouless transition [18], but this is out of scope of the present paper. However, having strong intersite excitonic liquid fluctuations could cause the irreducible charge vertices to exhibit precursor features, and it could be that our finding above is a signal of such an impending instability. More work is certainly needed to put this idea on a stronger footing, but this requires a separate investigation.

Finally, one would expect emergence of anomalous features in vertex functions and charge fluctuations close to the MIT to have deeper ramifications. Specifically, we now address the question outlined in the Introduction: "Can we study the long-time response of the FKM to a sudden local quench, and can such an endeavor provide deeper insight into the 'strong' localization aspect inherent in a continuous 'Mott' transition?" In other words, if we introduce a local, suddenly switched-on potential in the manner of a deep core hole potential in metals, how would the long-time response of the "core hole" spectrum evolve with U? In the famed instance of a Landau Fermi-liquid metal, the seminal work of Anderson [19] and Nozieres and de Dominicis [20] leads to the result that at long times the core hole propagator, related to the wave-function overlap between the ground states without and with the suddenly switched potential, goes like a power law, $\rho_h(t)|_{t\to\infty} \simeq t^{-\alpha}$ with $\pi\alpha = \tan^{-1}[V_h \rho_c(0)]$ being the (s wave for a local scalar potential) scattering phase shift. It has also long been shown that [21] the deep reason for this feature is that the particle-hole fluctuation spectrum, $\rho_{ph}(\omega)$ (related to the collective charge fluctuation response), in a Fermi gas is linear in energy. Explicit evaluation of the core hole response when e-e interactions in the Landau Fermi-liquid sense are present is a much more involved and delicate matter [14]. It is clear that qualitative change(s) in the low-energy density fluctuation spectrum must qualitatively modify the long-time response to such a sudden quench.

Answering this question in our case of the FKM is a subtle matter, since the c-fermion spectral function is *not* that of a Landau Fermi liquid, but describes an incoherent non-Landau Fermi-liquid state. As long as $\mathrm{Im}\chi_{ch}(\omega) \simeq \omega$ holds, however, we expect that the long-time response will be similar to that evaluated by Janis and Pokorny [14] using rather formal Wiener-Hopf techniques. Ultimately, the long-time response

still behaves in a qualitatively similar way to that for the free Fermi gas, except that the exponent in the power law is modified by interactions [thus, $\mathrm{Im}\chi_{ch}(\omega) \simeq \omega$ still holds, but with sizable renormalization]. In our case, we thus expect that $\rho_h(t)|_{t\to\infty} \simeq t^{-\alpha}$ still holds for $U < 1.3$, since we do find $\mathrm{Im}\chi_{ch}(\omega) \simeq \omega$ in this regime in the infrared. However, the qualitative change to the form $\mathrm{Im}\chi_{ch}(\omega) \simeq \omega^{1-\kappa}$ with $0 < \kappa < 1$ in the infrared for $U \geqslant 1.4$ must also qualitatively modify the long-time overlap and the core hole response.

Rather than resort to a direct computation of the long-time response within CDMFT, we will find it more instructive to consider this issue by using the low-energy results gleaned from CDMFT as inputs into an elegant approach first used in the context of the seminal x-ray edge problem by Schotte and Schotte [22] and by Müller-Hartmann *et al.* [21]. To this end, we have to identify the collective charge fluctuations encoded in $\chi_{ch}(\omega)$ with a bath of bosonic particle-hole excitations in the incoherent metal. Generally, using the linked cluster expansion, the spectral function of the localized core hole is

$$S_h(\omega) = \frac{1}{2\pi}\int_{-\infty}^{\infty} dt e^{i\omega t} \times \exp\left[V_h^2 \int_0^{\infty} dE \mathrm{Im}\chi_{ph}(E)\frac{e^{-iEt}-1}{E^2}\right] \quad (24)$$

where V_h is the "suddenly switched" core hole potential. As long as $\mathrm{Im}\chi_{ph}(E) \simeq E$, we estimate, similar to the well-known result, that the core hole spectral function behaves like $S_h(\omega) \simeq \omega^{-\alpha}$ with $\alpha = (1/\pi)\tan^{-1}[V_h\rho_{00}(0)]$, with $\rho_{00}(0)$ being the CDMFT LDOS at the Fermi energy [in a full computation, this exponent will change a bit because $\rho_{00}(\omega)$ has sizable frequency dependence close to $\omega = 0$ at strong coupling in the metal as found in Results, but the qualitative features will survive]. However, when $U \geqslant 1.4$, having Im $\chi_{ch}(\omega) \simeq \omega^{1-\kappa}$ must modify this well-known behavior. In this regime we find (see also Ref. [21]) the following leading contribution to the core hole spectral function:

$$S_h(\omega) \simeq \frac{V_h^2}{E_F}\left(\frac{E_F}{\omega}\right)^{1+\kappa} \exp\left[-\pi V_h^4\left(\frac{E_F}{\omega}\right)^{2(1-\kappa)}\right], \quad (25)$$

which is qualitatively distinct from the well-known form, and corresponds to a long-time wave-function overlap having a very nonstandard form: $\rho_h(t)|_{t\to\infty} \simeq e^{-t^{1-\kappa}}$. This qualitative modification of the long-time wave-function overlap is a strong manifestation of a type of localization at work. It would be tempting to associate this with a many-body localized regime, especially since the Landau quasiparticle picture is also violated within this strong-coupling regime, but more work is called for to clinch this issue. The basic underlying reason for this behavior is the same as the one leading to generation of the anomalous exponent κ in the p-h fluctuation spectrum, i.e., strong ω dependence and incipient nonanalyticity in the irreducible p-h vertex close to the MIT.

VI. DISCUSSION AND CONCLUSION

Using the disordered binary alloy analogy extended to a two site cluster, we have investigated $1/d$ effects on the continuous MIT in the "simplified" FKM (by this, we mean a FKM where the disorder is quenched, rather than annealed, so quantities like $\langle x_0\rangle$ and $f_{0\alpha}$ are fixed and given from a binary distribution, rather than computed self-consistently, as in the true FKM). In spite of this simplification, we find that quantum critical features at the level of one-electron Green's functions and self-energies are very similar to those obtained from an "Anderson-Falicov-Kimball" [14] model. This is not so surprising, since the effect of the FK term $U\sum_i n_{id}n_{ic}$ is precisely to generate a band "splitting" for all U in the FKM as well, and a binary alloy disorder indeed has exactly a similar effect on the DOS. Thus, within DMFT or CDMFT approaches such as ours, one would expect quantitative changes in the spectral functions, but no qualitative modification of critical exponents in the LDOS exactly at the band splitting Hubbard-like transition.

However, in strong contrast to the one-electron response, inclusion of the *nonlocal* irreducible p-h vertex in computation of the dynamic charge susceptibility does lead to significant effects at strong coupling. We have shown that $\mathrm{Im}\chi_{ch}(\omega) \simeq \omega^{1-\kappa}$ with $0 < \kappa < 1$ occurs precisely in the same regime where the nonlocal vertex shows strong frequency dependence and signs of an impending nonanalyticity (the latter occurs either at the MIT or precedes it; see above). This feature is quite anomalous, indicating that an unusual collectively fluctuating state of the electronic fluid, characterized by infrared critical *bosonic* p-h modes, sets in before the MIT occurs. Naturally, one expects that this feature will drastically modify the charge responses in the strong-coupling limit: in fact, related effects should reveal themselves in optical response of the disordered electron fluid. We leave detailed elucidation of such points for future work.

To summarize, we have analyzed the role of short-ranged (spatially nonlocal) alloy correlations on the Hubbard-like MIT in a binary disorder Anderson model at strong coupling in detail. While quantum critical features at the one-electron level are exactly similar to recent DMFT results [14] for the disordered FKM, nonlocal vertex corrections show up rather dramatically as a qualitative change in character of the collective p-h spectrum at strong coupling. In contrast to previous CPA studies, this is a concrete manifestation of the relevance of dynamical effects associated with $1/d$ alloy correlations near the quantum critical point associated with a continuous MIT of the Hubbard band splitting type. It is obviously of interest to elucidate the nature and consequences of this strong-coupling QCP in various transport responses. This aspect is under study, and will be reported separately.

ACKNOWLEDGMENTS

We are grateful to Prof. T. V. Ramakrishnan for insightful discussions.

[1] P. W. Anderson, Phys. Rev. **109**, 1492 (1958).
[2] J. Kroha, Physica A (Amsterdam) **167**, 231 (1990), and references therein.
[3] S. Mahmoudian, S. Tang, and V. Dobrosavljevic, Phys. Rev. B **92**, 144202 (2015), and references therein.
[4] R. Mills and P. Ratanavararaksa, Phys. Rev. B **18**, 5291 (1978).

[5] M. Jarrell and H. R. Krishnamurthy, Phys. Rev. B **63**, 125102 (2001).
[6] D. A. Rowlands, J. B. Staunton, and B. L. Gyorffy, Phys. Rev. B **67**, 115109 (2003).
[7] J. Hubbard, Proc. R. Soc. A **277**, 237 (1964).
[8] V. Khemani, R. Nandkshore, and S. Sondhi, Nature Physics **11**, 560 (2015).
[9] Y. Gefen, R. Berkovits, I. V. Lerner, and B. L. Altshuler, Phys. Rev. B **65**, 081106(R) (2002).
[10] M. S. Laad and L. Craco, J. Phys. Condens. Matter **17**, 4765 (2005).
[11] J. Freericks and V. Zlatic, Rev. Mod. Phys. **75**, 1333 (2003).
[12] A. Liebsch and N.-H. Tong, Phys. Rev. B **80**, 165126 (2009).
[13] P. vanDongen, K. Majumdar, C. Huscroft, and F. C. Zhang, Phys. Rev. B **64**, 195123 (2001).
[14] V. Janis and V. Pokorny, Phys. Rev. B **90**, 045143 (2014).
[15] T. Schafer, G. Rohringer, O. Gunnarsson, S. Ciuchi, G. Sangiovanni, and A. Toschi, Phys. Rev. Lett. **110**, 246405 (2013); G. Rohringer, A. Valli, and A. Toschi, Phys. Rev. B **86**, 125114 (2012).
[16] A. Georges, G. Kotliar, W. Krauth, and M. J. Rozenberg, Rev. Mod. Phys. **68**, 13 (1996).
[17] Hiroshi Shinaoka and Masatoshi Imada, Phys. Rev. Lett. **102**, 016404 (2009).
[18] V. Apinyan and T. K. Kopec, J. Low Temp. Phys. **176**, 27 (2014).
[19] P. W. Anderson, Phys. Rev. Lett. **18**, 1049 (1967).
[20] P. Nozieres and C. T. de Dominicis, Phys. Rev. **178**, 1097 (1969).
[21] E. Müller-Hartmann, T. V. Ramakrishnan, and G. Toulouse, Phys. Rev. B **3**, 1102 (1971).
[22] K.-D. Schotte and U. Schotte, Phys. Rev. **182**, 479 (1969).